Electronic structure of RuSr₂EuCu₂O₈ studied by x-ray absorption and photoemission spectroscopies

S. W. Han,[*] D. C. Ling,[†] H. M. Tsai,[‡] C. H. Chuang, S. L. Wu, and W. F. Pong[†]

Department of Physics, Tamkang University, Tamsui 251, Taiwan

J. W. Chiou

Department of Applied Physics, National University of Kaohsiung, Kaohsiung 811, Taiwan

M.-H. Tsai

Department of Physics, National Sun Yat-Sen University, Kaohsiung 804, Taiwan

L. Y. Jang, H. J. Lin, T. W. Pi, and J. F. Lee

National Synchrotron Radiation Research Center, Hsinchu 300, Taiwan

Local electronic structures of ruthenocuprate RuSr₂EuCu₂O₈ (RuEu-1212) were investigated by using x-ray absorption near-edge structure (XANES) and valence-band photoemission (VB-PES) measurements at room temperature, 80 K, and 25 K. The XANES results indicate that when RuEu-1212 is below Curie temperature, T_M, electrons are transferred not only from Cu $3d$ states, but also from Ru $4d$ states, to O $2p$ orbitals. Additionally, the partial spectral weight distributions derived from VB-PES measurements provide evidence of a weak overlapping between Ru $4d$ states and strongly Cu $3d$−O $2p$ hybridized states below the Fermi level, which results in a weak coupling between the CuO₂ and RuO₂ layers. The analysis of extended x-ray absorption fine structure shows that the appearance of weak ferromagnetism and superconductivity is accompanied by a significant decrease of dynamic local lattice distortions of high-shell Cu-Sr and Ru-Sr bonding in RuEu-1212.

I. INTRODUCTION

Coexistence of weak ferromagnetism (WFM) and superconductivity (SC) has been discovered in the 1212-type layered ruthenocuprates RuSr₂*R*Cu₂O₈ (Ru*R*-1212, *R* = Gd, Eu).[1,2] Over the last decade, much attention has been paid to examine how WFM and SC accommodate each other on a microscopic scale.[1–4] The crystal structure of Ru*R*-1212 is similar to that of superconducting YBa₂Cu₃O₇ (YBCO) with the replacement of the Cu-O chains by two-dimensional Ru-O layers, in which Ru is octahedrally coordinated with four O$_{Ru−plane}$ and two O$_{apical}$ ions.[5] The RuO₆ octahedra, collectively rotated by approximately 14° around the *c* axis,[6] are connected through an O$_{apical}$ ion to four Cu-coordinated O$_{Cu}$ ions to form a CuO₅ pyramid structure (see Fig. 1).[7] Neutron diffraction studies suggested that the magnetic ordering is principally in a canted *G*-type antiferromagnetic (AFM) ordering of the Ru magnetic moments with a weak ferromagnetic ordering within the Ru-O planes.[5,8] These Ru*R*-1212 materials generally have superconducting temperatures (T_c) and Curie temperatures (T_M) in the range of 30–50 K and 130–140 K, respectively, and are sensitively dependent on sample preparation conditions.[9,10] The Ru ion was assumed to be pentavalent (d^3 or $t_{2g}{}^3 e_g{}^0$ configuration) in these compounds. It was argued that, if the Ru ion is less than pentavalent in these compounds, charge transfer or hole doping from the Cu-O layers would be expected to occur because the partially occupied t_{2g} band of the perovskite Ru-O layers would cross the e_g Hubbard band of the Cu-O layers.[6,11] The electronic properties of both Ru-O and Cu-O layers would be expected to involve itinerant−electron-like behavior, while the Cu-O and Ru-O layers may show SC and WFM properties, respectively. The coexistence of WFM and SC

phases in RuGd-1212 has also been elucidated by full-potential linearized augmented plane-wave (FLAPW) calculations.[12,13] Therefore, determining the valences of Ru and Cu ions and the electronic structures of Ru*R*-1212 is important to understand the coexistence of magnetic and superconducting properties. However, despite extensive studies described above, how the SC phase emerges in the presence of a WFM state is still a matter of debate. To better understand these issues, x-ray absorption near-edge structure (XANES) and valence-band photoemission spectroscopy (VB-PES) measurements were performed on RuEu-1212. Partial spectral weights (PSW)[14] of the Ru $4d$, Cu $3d$, and O $2p$ states were derived from VB-PES spectra by taking advantage of the large differences between photon-energy-dependent photoionization cross sections of Ru $4d$, Cu $3d$, and O $2p$ orbitals in RuEu-1212.[15] The XANES measurements and PSW distributions provide direct evidence that Ru $4d$ and Cu $3d$-O $2p$ hybridized states at/below the Fermi level (E_f) are weakly coupled in RuEu-1212.

II. EXPERIMENTAL

All XANES and VB-PES experiments were performed at the National Synchrotron Radiation Research Center in Hsinchu, Taiwan. The XANES spectra were obtained at the high-energy spherical grating monochromator-20A, wiggler-17C, double-crystal monochromator-15B, and Dragon-11A beamlines at room temperature (RT), 80 K, and 25 K using fluorescence yield mode (fluorescence yield is bulk sensitive enough to avoid surface contaminations) at a base pressure in the low range of 10^{-9} torr at RT. The samples were mounted in a closed-cycle helium cryostat for temperature-dependent
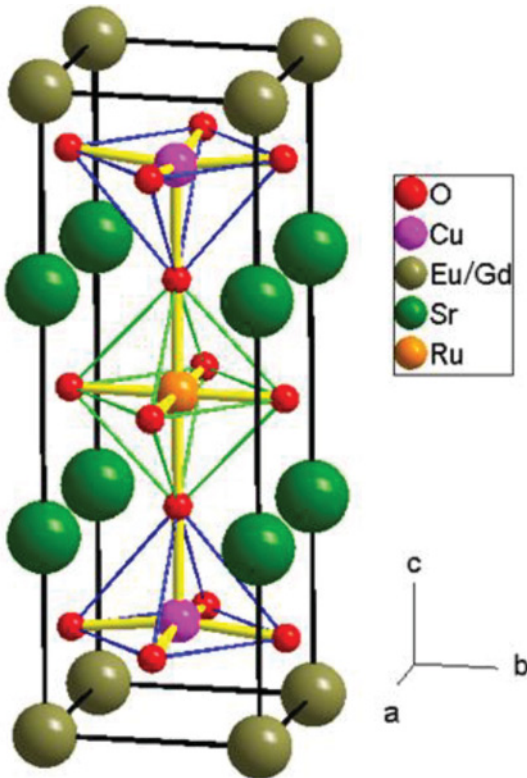
FIG. 1. (Color online) Crystal structure of RuEu-1212 with a tetragonal *P*4/*mbm* space group.

measurements. The VB-PES measurements were performed with a hemispherical energy analyzer at the low-energy spherical monochromator-8A beamline at a base pressure $\sim 5 \times 10^{-10}$ torr at RT. The polycrystalline RuEu-1212 and reference $SrRuO_3$ (SRO) samples were prepared by the

standard solid-state reaction method and were scraped *in situ* using a diamond file in vacuum to obtain the clean surface before VB-PES measurements were made. X-ray diffraction pattern verifies that the crystal structure of RuEu-1212 has a tetragonal *P*4/*mbm* space group presented in Fig. 2(a). The temperature dependencies of resistivity and dc magnetization were measured by physical property measurement system for RuEu-1212 and SRO, respectively, as shown in Fig. 2(b). It demonstrates the coexistence of SC and WFM phases in RuEu-1212 with $T_c \sim 35$ K and $T_M \sim 130$ K. The reference SRO is also found to be a metallic ferromagnet with $T_M \sim 160$ K, in agreement with the previous report.[16]

III. RESULTS AND DISCUSSION

Figure 3(a) presents the O *K*-edge XANES spectra of the RuEu-1212 and SRO samples at 25 K, 80 K, and RT. All these spectra were normalized in the energy range between 550 and 560 eV (not fully shown in the figure) after subtracting the background. Three major near-edge features in the spectra of RuEu-1212, labeled as a_1 to c_1, are centered at $\sim$528.0, 529.5, and 531.5 eV, respectively. These features provide detailed information about unoccupied O $2p$-derived states or hole concentration of O $2p$ character commonly observed in perovskite oxides and ruthenocuprates.[17–22] The general line shapes of the features a_1–c_1 of RuEu-1212 differ significantly from those of reference SRO, all of which are magnified in Fig. 3(b) with the subtraction of the background shown by a dotted line. Features a_1–c_1 can be mainly attributed to O $2p$-Ru $4d$ hybridized states with a very small contribution from O $2p$-Cu $3d$ hybridized states according to theoretical calculations by Nakamura *et al.* for RuGd-1212.[12,13] Specifically, feature a_1 is primarily associated with the Ru t_{2g} band and the broad features (between features b_1 and c_1) can be ascribed to the
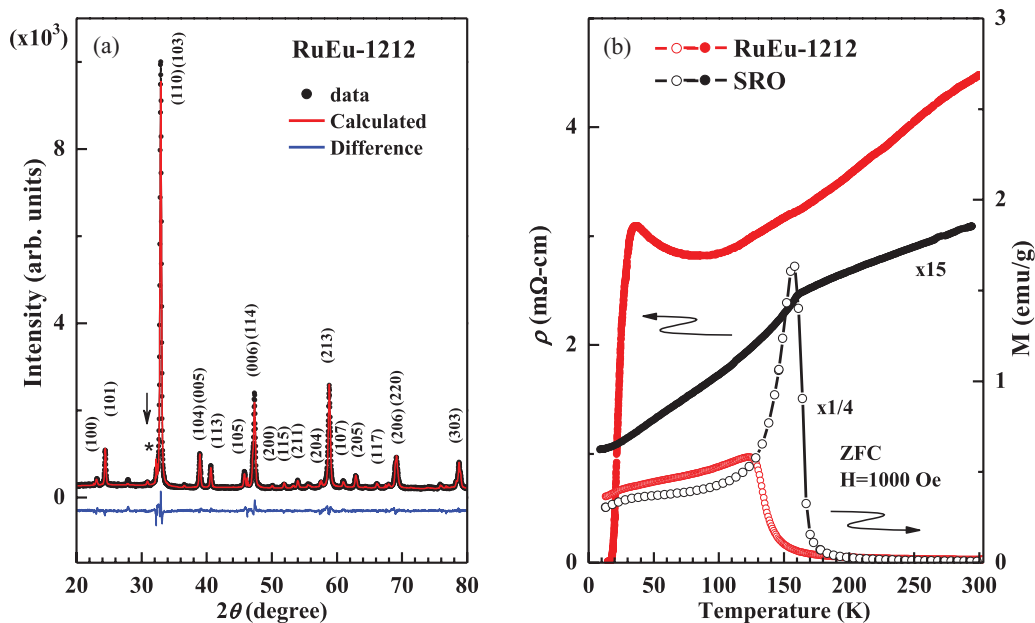

FIG. 2. (Color online) (a) X-ray diffraction pattern of the RuEu-1212 sample. The <5% SRO impurity phase is indicated by the downward arrow. The crystal structure of RuEu-1212 is refined by the Rietveld program with the weighted profile *R*-factor $R_{wp} = 6.17\%$. (b) Comparison between resistivity (left) and zero-field-cooled (ZFC) dc magnetization of 1000 Oe (right) of the RuEu-1212 and SRO samples.
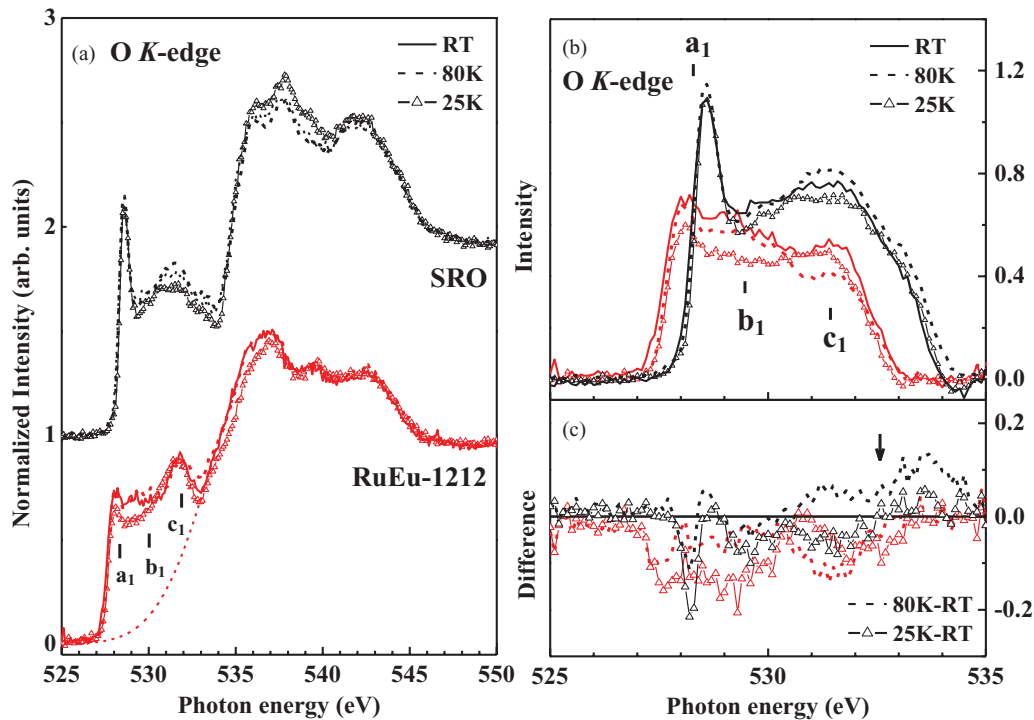
FIG. 3. (Color online) (a) Normalized O K-edge XANES spectra of RuEu-1212 (red/dark gray) and SRO (black) at 25 K, 80 K, and RT. (b) Magnified near-edge features after subtraction of background. (c) Difference intensities of O K-edge near-edge features of RuEu-1212 and SRO between 25 K/80 K and RT.

Ru e_g band. The energy separation between the Ru t_{2g} band ($\sim$528 eV) and the center of the e_g band ($\sim$531 eV) (with a crystal field splitting, $\Delta = 10$ D$_q$) is approximately 3 eV in agreement with that obtained from the Ru L_3-edge XANES spectra to be shown later. Additionally, the general line shapes at the O K edge for SRO are similar to those reported in the literature[16,19–22] and were observed to be composed of a single feature at $\sim$528.5 eV and broad features in the region of 529–534 eV, which correspond mainly to Ru $4d$ t_{2g} and e_g states. Clearly, O K-edge XANES features of RuEu-1212 shift overall to lower energies, and their intensities are smaller than those of SRO regardless of whether the temperature is decreased from RT to 80 K and then to 25 K. Figure 3(c) displays difference intensities of O K-edge near-edge features of RuEu-1212 between 25 K/80 K and RT; the overall negative difference intensities shown in Fig. 3(c) reveal a decrease in the number of unoccupied O $2p$ states in RuEu-1212 as the temperature is reduced from RT to 80 K and 25 K. These effects are strongly related to the magnetic property of Ru ions and the SC property in RuEu-1212. As indicated above, features **a**$_1$–**c**$_1$ are primarily associated with Ru t_{2g} and e_g states. A decrease in the number of unoccupied O $2p$ states in RuEu-1212 implies an increase of the occupation of O $2p$ derived states and may suggest electron transfer from Cu $3d$ orbitals in the Cu-O layers through O$_{apical}$ p orbitals to the Ru-O layers. In contrast, positive difference intensities of the features in the region 530–535 eV between 80 K and RT are observed for SRO as shown in Fig. 3(c).

Figure 4(a) and the inset display Cu $L_{3,2}$-edge XANES spectra at RT, 80 K, and 25 K and difference intensities of the features in these spectra between 25 K/80 K and RT,

respectively, to verify the transfer of electrons from Cu $3d$ orbitals in the Cu-O layers through O$_{apical}$ p orbitals to the Ru-O layers when the temperature is reduced from RT to 80 K and 25 K, accompanied by the change in phase from paramagnetism (PM) to WFM and then to SC. According to dipole-transition selection rules, the dominant transition is from Cu $2p_{3/2}$ and $2p_{1/2}$ to unoccupied Cu $3d$ states. The area under the white line in the Cu $L_{3,2}$-edge XANES spectra is predominately a convolution of the absolute square of the transition matrix element and the density of unoccupied Cu e_g states because Cu t_{2g} states are almost fully occupied. The inset of Fig. 4(a) shows that the overall integrated intensity (from 928–945 eV) between 80 K and RT and between 25 K and RT are positive and negative, respectively. It reveals that the number of unoccupied states or hole concentration in the Cu e_g band increased (decreased) as the temperature is reduced from RT to 80 K (25 K). The 80 K vs RT result implies that when the RuEu-1212 sample is at a temperature below T_M and its phase changed from PM to WFM, electrons are transferred from Cu e_g states in the Cu-O layers to the Ru-O layers through O$_{apical}$ p orbitals. In contrast, difference Cu L_3-edge XANES intensities between 25 K and RT are mostly negative, suggesting that as the RuEu-1212 sample is in the SC phase ($T < T_c$), the overall number of unoccupied states or hole concentration in the Cu e_g band decreases relative to that in the PM phase at RT. Although the large intensity changes observed at the Cu L_3-edge XANES spectra upon the lowering of the temperature, as shown in Fig. 4(a), were argued to be due to the correlation effects, with which the Cu $3d$ counts might not be altered and additional holes in the Cu-O layers might be shifted to the O sites, the CuO$_5$ lattice
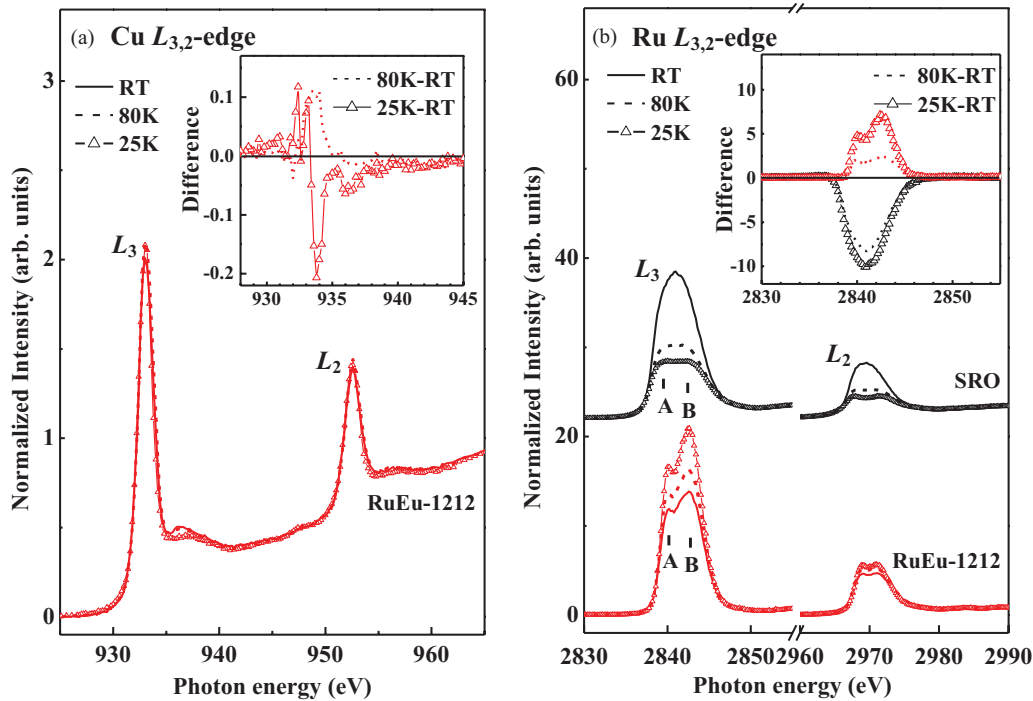
FIG. 4. (Color online) (a) Cu $L_{3,2}$-edge XANES spectra; inset shows difference spectra of Cu L_3-edge near-edge features of RuEu-1212 between 25 K/80 K and RT. (b) Ru $L_{3,2}$-edge XANES spectra; inset shows difference spectra of Ru L_3-edge near-edge features of RuEu-1212 and SRO between 25 K/80 K and RT.

distinction (in particular, the displacement of apical O atom) could tune orbital hybridization substantially and give rise to intensity changes at the Cu $L_{3,2}$-edge XANES upon lowering the temperature. Figure 4(b) and the inset display Ru $L_{3,2}$-edge XANES spectra at RT, 80 K, and 25 K and difference Ru L_3-edge intensities between 25 K/80 K and RT, respectively. The area under the white line in the Ru $L_{3,2}$-edge XANES spectra is dominantly associated with the transition from Ru $2p_{3/2}$ and $2p_{1/2}$ to unoccupied Ru $4d$ states. The Ru L_3-edge absorption spectrum of SRO has two features (A and B), which are attributable to transition from Ru $2p_{3/2}$ to unoccupied Ru $4dt_{2g}$ and e_g states,[22,23] respectively. The two well-resolved features A ($\sim$2840 eV) and B ($\sim$2843 eV) are also observed in the spectrum of RuEu-1212, and its crystal field splitting ($\Delta =$ 10 D$_q$) is approximately 3 eV, in consistence with O K-edge XANES results shown in Fig. 3. The inset of Fig. 4(b) shows that the Ru L_3-edge XANES intensities of RuEu-1212 increase with decreasing temperature from RT to 80 K and then to 25 K, indicating that the number of unoccupied Ru $4d$ states or the concentration of holes in those states increases as temperature decreases. This fact further reveals that when RuEu-1212 is at a temperature below T_M, electrons are not only transferred from Cu $3d$ states in the Cu-O layers, but also from the Ru $4d$ states to O $2p$ orbitals in the Ru-O layers. In contrast, the intensities of the features in the Ru L_3-edge XANES spectra of SRO, shown in the inset of Fig. 4(b), decreases with decreasing temperature down to 25 K. It indicates that Ru ions gain rather than lose electrons in SRO. This opposite result suggests that the Cu-O layers may play an important role in causing Ru ions to lose electrons in RuEu-1212. Another scenario associated with this finding is either different magnetic structure between

RuEu-1212 (WFM) and SRO (FM) at low temperatures or the presence of Ru $4d$ orbital ordering in SRO proposed by LDA+U calculations.[24] It is worth noting that there is a strong intensity change in the Ru L_3-edge XANES spectrum of SRO when the temperature was lowered from RT to 80 K/25 K, as shown in Fig. 4(b), similar to the properties of the Cu L_3-edge XANES spectra stated previously, which can be also caused by lattice distortion in the RuO$_6$ networks in the perovskite ruthenates. Such electron-lattice interaction is strongly correlated with the O $2p$ and Ru $4d$ hybridization, which can be attributable to the extended character of the Ru $4d$ orbitals in the states near/at E_f. The small structural variation can affect hybridization between Ru $4d$ and O $2p$ orbitals and charge transfer. Both theoretical calculations and experimental measurements for SRO showed a strong O $2p$-Ru $4d$ hybridization throughout the valence-band and conduction-band regions at/near E_f.[25,26] The lattice distortion of the RuO$_6$ networks in SRO can be slightly reduced with decreasing temperature, which affects p-d hybridization moderately but alters spectral intensity of the Ru L_3-edge strongly at $T < T_M$.

Figure 5(a) displays VB-PES spectra of RuEu-1212 and SRO at/below E_f obtained at various photon energies from $h\nu = 35$ to 150 eV, including the Ru $4p \rightarrow 4d$ resonant excitation threshold near 54 eV.[27] Each spectrum is normalized to its maximum height for comparison. The general line shapes of the VB-PES spectra of RuEu-1212 with various photon energies differ significantly from that of reference SRO. The main VB-PES spectra of RuEu-1212 clearly shift to lower binding energies relative to that of SRO. As mentioned earlier, the RuEu-1212 and SRO samples were scraped *in*
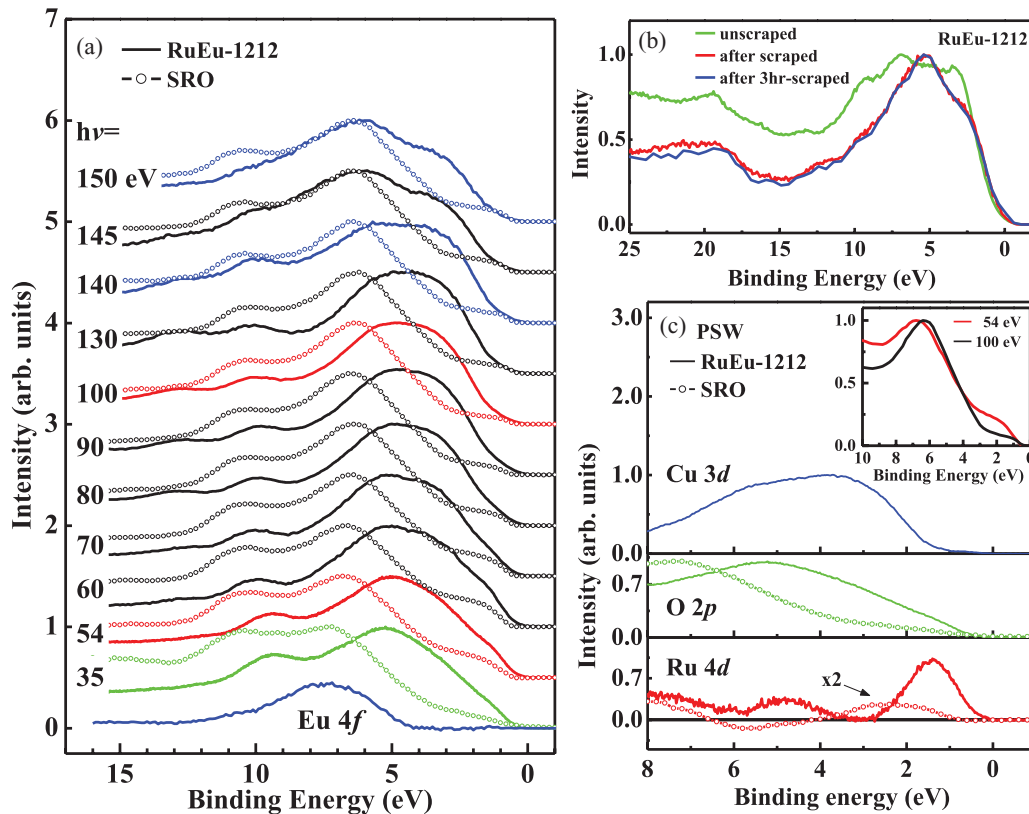
FIG. 5. (Color online) (a) VB-PES of RuEu-1212 (solid line) and SRO (open-circle line) obtained at various photon energies between 35 and 150 eV. The feature in the bottom blue (medium gray) spectrum represents contribution from PSW of Eu 4f states. (b) Displays of the VB-PES spectra of RuEu-1212 obtained at photon energy of 150 eV in the cases of unscraped (green/gray), after-scraped (red/dark gray) and after 3 hr-scraped (blue/medium gray) at RT. (c) Deduced PSW of Cu 3d, O 2p, and Ru 4d states for RuEu-1212 (solid line) and O 2p and Ru 4d states (The intensity has been scaled by a factor of 2) for SRO (open-circle line). The VB-PES spectra of SRO at/near E_f at incident energy of 54 eV (red/dark gray) and 100 eV (black) are expanded in the upper inset of figure.

situ using a diamond file in vacuum to obtain the clean surface before VB-PES measurements were made. However, the sample cleaning methods (scraping[19] vs annealing[20]) have been considered to be very robust in many highly correlated systems, which often leads to controversial results. To verify that the samples were free from surface contamination during VB-PES measurements, VB-PES spectra of the RuEu-1212 samples prepared under various cleaning conditions, namely unscraped, after scraped, and after 3-hr scraped, obtained at photon energy of 150 eV were displayed in Fig. 5(b). The line shapes and intensities of the VB-PES spectra of the samples prepared under the after- and after-3-hr-scraped cleaning conditions are essentially identical, and they are quite different from that of the unscraped one, which indicated that scraping has already eliminated surface contamination shown in the spectrum of the unscrapted sample. These results demonstrate that the scraped samples prepared in a base vacuum of $\sim$5 $\times$ 10^{-10} torr can keep contamination within a reasonable level during measurements. The dependence of the valence-band line shape on the photon energy can be used to derive PSW distributions of various electronic states of a given constituent element in the compound.[14,20] The Cooper minimum phenomenon of the Ru 4d photoionization cross section and the Eu 4d → 4f resonant excitation occur at photon energies $h\nu$ = 100 and 150 eV,[28] respectively. The

bottom blue spectrum in Fig. 5(a) shows difference intensities between on-resonance ($h\nu$ = 150 eV) and off-resonance ($h\nu$ = 140 eV) VB-PES spectra, which represents PSW distribution of Eu 4f states. This PSW distribution has a feature centered at $\sim$7 eV and has no appreciable PSW at/near E_f. Beside Eu 4f states, PSW distributions of Ru 4d, Cu 3d, and O 2p states are also qualitatively determined to elucidate the electronic structures at/below E_f of RuEu-1212. If Ru^{5+}, Cu^{2+}, and filled O 2p bands (2p^6) are assumed and Eu 4f states are ignored, the O 2p : Cu 3d : Ru 4d cross-sectional ratio in RuEu-1212 is $\sim$85% : 14% : 1% at $h\nu$ = 35 eV, $\sim$71% : 25% : 4% at $h\nu$ = 54 eV and $\sim$52% : 48% : 0% at $h\nu$ = 100 eV,[15] which shows that O 2p states contribute most to the $h\nu$ = 35 eV spectrum. Generally, the photoionization cross section of Ru 4d electrons increases in proportion to the photon energy, except at the Cooper minimum of $h\nu$ = 100 eV for Ru 4d, at which the cross sections of O 2p and Cu 3d photoelectrons become comparable. If one subtracts O 2p PSW distribution contained in the $h\nu$ = 35 eV spectrum from that in the $h\nu$ = 100 eV spectrum, the Cu 3d PSW distribution will become dominant in the adjusted $h\nu$ = 100 eV spectrum, and the Cu 3d PSW distribution can be roughly determined. By the same way, the PSW distribution of the Ru 4d states can be qualitatively derived by subtracting PSW distributions of O 2p and Cu 3d states from the $h\nu$ = 54 eV VB-PES spectrum because, at

$h\nu = 54$ eV, the cross section of Ru $4d$ photoelectrons is larger than those at other photon energies due to the resonance effect. Figure 5(c) presents PSW distributions of Ru $4d$, Cu $3d$, and O $2p$ states of RuEu-1212 at/below E_f. The PSW's of O $2p$ and Cu $3d$ states spread over a wide range of energies below E_f with insignificant PSW at/near E_f, indicative of a strong hybridization between Cu $3d$ and O $2p$ orbitals well below E_f and no significant partial DOSs at/near E_f, which implies a smaller amount of hole concentration in the CuO$_2$ layers than that of optimally doped YBCO. This finding suggests that RuEu-1212 is an underdoped superconductor.[29] The feature in the PSW distribution of the Ru $4d$ states shown in the bottom panel of Fig. 5(c) centered at $\sim$1.5 eV below E_f is relatively narrow with a full width at half maximum of $\sim$1.3 eV, which indicates that the Ru $4d$ states are relatively localized. The PSW distributions deduced from VB-PES spectra indicate that the Ru $4d$ band lies much closer to E_f than the Cu $3d$ band, which suggests that the former may play a more important role in determining the physical properties of RuEu-1212. It is well documented in the literature that superconductivity in cuprates is generally caused by Cu $3d$-O $2p$ hybridized states lying at/near E_f.[30,31] For the case of ruthenates, the VB-PES spectra of SrRu$_{1-x}$Mn$_x$O$_3$ show prominent DOSs at/near E_f, which are contributed mostly from Ru $4d$ orbitals.[23] The analysis of the VB-PES spectra and PSW distributions of RuEu-1212 indicates that Ru $4d$ states are much closer to E_f than Cu $3d$ and O $2p$ states in agreement with band-structure calculations,[12,13] which suggested that Ru t_{2g} states have insignificant interactions with Cu e_g states at/near E_f in RuEu-1212. Decoupling between Cu-O and Ru-O layers has been reported theoretically[3] and experimentally.[32] In addition, the PSW distribution of the Ru $4d$ states shows a satellite feature with a smaller intensity at the binding energy of $\sim$5 eV below E_f. This feature may arise from a weak hybridization between Ru $4d$ and O $2p$ states, which has a maximum PSW at about 5.2 eV below E_f, as shown in the Fig. 5(c). Another possible origin is that the contributions of Cu $3d$ and O $2p$ PSW's might not be completely eliminated in the deduced PSW distribution of the Ru $4d$ states due to the fact that it is roughly determined by subtracting the PSW distribution of the O $2p$ states in the $h\nu = 35$ eV VB-PES spectrum and that of the Cu $3d$ states in the $h\nu = 100$ eV VB-PES spectrum. On the other hand, the O $2p$ PSW distribution in the case of SRO can be regarded as contributed from the $h\nu = 100$ eV spectrum at the Cooper minimum of Ru $4d$ orbitals, and Ru $4d$ PSW distributions can be qualitatively obtained by subtracting this spectrum from the $h\nu = 54$ eV spectrum, to which the Ru $4d$ contribution is large due to the resonance effect.[20] The enhanced Ru $4d$ states at/near E_f in the $h\nu = 54$ eV spectrum relative to those in the $h\nu = 100$ eV spectrum can be clearly seen at the upper inset of Fig. 5(c). The feature centered at $\sim$3 eV below E_f in the PSW distribution of the Ru $4d$ states in SRO, as also shown in the bottom of Fig. 5(c), is relatively broader with a full width at half maximum of $\sim$2.5 eV, which indicates that the Ru $4d$ states in SRO are comparatively more delocalized than those in RuEu-1212 and shows a highly hybridization between Ru $4d$ and O $2p$ at/near E_f in SRO as well.[19,20]

It has been argued that when the Ru t_{2g} band of the Ru-O layer crosses the Cu e_g band of the Cu-O layer and the Ru

ion is less than pentavalent in RuR-1212, transfer of electron charge from the Cu-O to Ru-O layers is expected to occur.[6,11] Hence, the valences of the Cu and Ru ions can be written as Cu$^{2+\delta}$ and Ru$^{5-2\delta}$, respectively, where δ is the amount of electron charge transferred between the Cu-O and Ru-O layers. This charge transfer introduces δ holes into the Cu e_g band of the Cu-O layers and 2δ electrons into the minority-spin Ru t_{2g} band of the Ru-O layers, which was argued to be mainly responsible for SC and WFM phases in RuR-1212, respectively. However, present XANES results demonstrate that, when the temperature of RuEu-1212 is below T_M, the electrons are transferred not only from Cu $3d$ states in Cu-O layers but also from the Ru $4d$ states to O $2p$ orbitals. Furthermore, when the temperature is lower than T_c, the overall number of unoccupied states or the hole concentration in the Cu e_g band is lower than that in the PM phase at RT. It is known that the peak position and the intensity ratio between Ru L_2 and L_3 edge can be relevant parameters, bearing proportionality with the Ru valency in ruthenocuprates.[33] However, the general line shapes and spectral intensities observed at the transition-metal (TM) $L_{3,2}$-edge XANES spectra are rather complicated and exhibit strong multiplet caused by the crystal field and intra-atomic Coulomb repulsion.[34] Therefore, the threshold energy position of the TM K-edge XANES spectra are commonly used to determine the valence of TM atoms in TM-related compounds. The thresholds of the Cu K-edge XANES spectra of Cu oxides with a Cu$^{2+\delta}$ charge state have been observed to shift to higher energy relative to that of Cu^{2+} if δ is not too small.[17] However, no energy shift was observed in the Cu K-edge XANES spectra of RuEu-1212 relative to that of CuO (Cu^{2+}) at temperatures from RT down to 25 K, as illustrated in Fig. 6(a), suggestive of a small δ value. As for the Ru charge state, the thresholds of the Ru K-edge XANES spectra of RuEu-1212 have higher energies ($\sim$2.2 eV) than that of SRO (Ru^{4+}), although both thresholds are insensitive to the temperature between RT and 25 K, as shown in Fig. 6(b). The shifted thresholds at the Ru K edge suggest that Ru ions in RuEu-1212 have an effective (average) charge between +4 and +5, although a previous Ru L_3-edge XANES study reported that the Ru valence in ruthenocuprates (Ru, M = Sn, Nb)Gd-1212 with fixed-valent cations Nb^{3+} and Sn^{4+} on the Ru site is about 4.8.[33] The above results suggest a need for further investigations on the charge state of the Ru ions (in the RuO$_2$ layers) and charge transfer/hole doping (in the CuO$_2$ layers) in RuR-1212 compounds.

As mentioned previously, the crystal structure of RuEu-1212 is similar to that of superconducting YBCO with the replacement of the Cu-O chains by the Ru-O layers, which leads to tilts and rotations of the RuO$_6$ octahedra by about 14° around the c axis, and the magnetic ordering in RuEu-1212 was argued to be a canted G-type AFM ordering of the Ru magnetic moments with a WFM ordering within the Ru-O plane.[5,6] The electronic and magnetic properties of high-T_c superconducting cuprates are sensitive to local distortions of the Cu-O pyramid, which prompted investigations of the electron-lattice interactions and lattice distortions in these materials.[35,36] RuEu-1212 is expected to have similar properties, and it is worth investigating its local atomic structures at the Ru and Cu sites. Figures 7(a)–7(c) display the Fourier
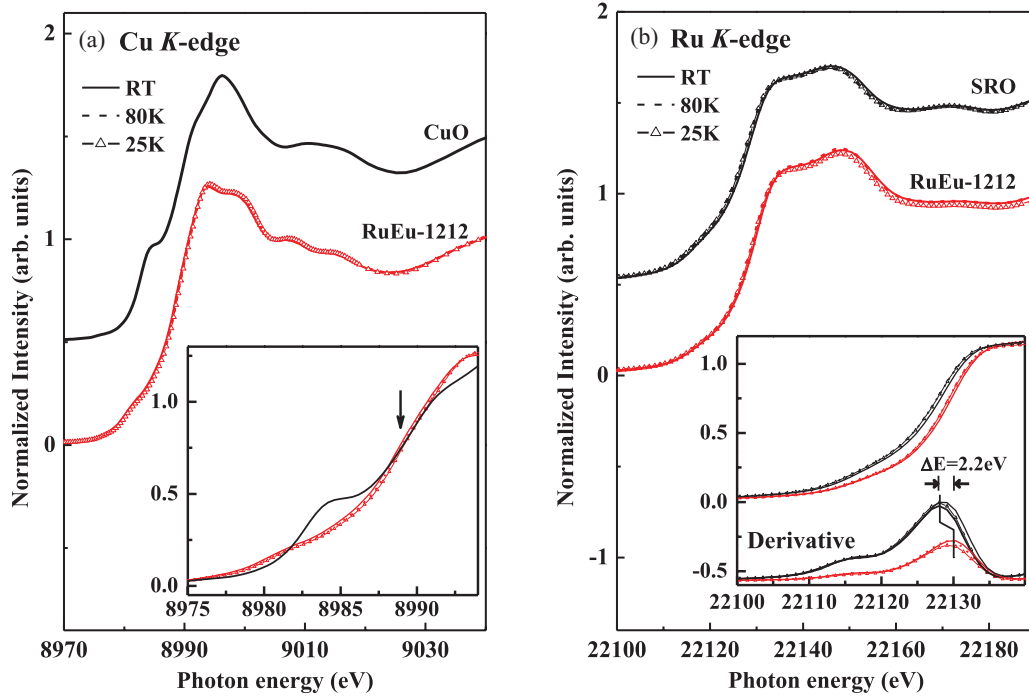
FIG. 6. (Color online) (a) Cu K-edge XANES features of RuEu-1212 and CuO at RT, 80 K and 25 K. Lower inset; magnified near-edge features. (b) Ru K-edge XANES features of RuEu-1212 and SRO at RT, 80 K, and 25 K. Lower inset: magnified near-edge features and their first derivatives.

transform (FT) of Cu and Ru K edge and their corresponding extended x-ray absorption fine structure (EXAFS) $k^3\chi$ data of RuEu-1212 at RT, 80 K, and 25 K, respectively.[37] It reveals that the general line shapes and the radial distribution of the FT spectra at Cu and Ru K edges at low temperatures

(80 and 25 K) of RuEu-1212 are similar to those at RT, which demonstrate that the overall local atomic structures at Cu and Ru sites at RT (PM phase) and low temperatures (WFM and SC phases) are similar. The intensities of the first main features in the FT spectra at the Cu (Ru) K edge
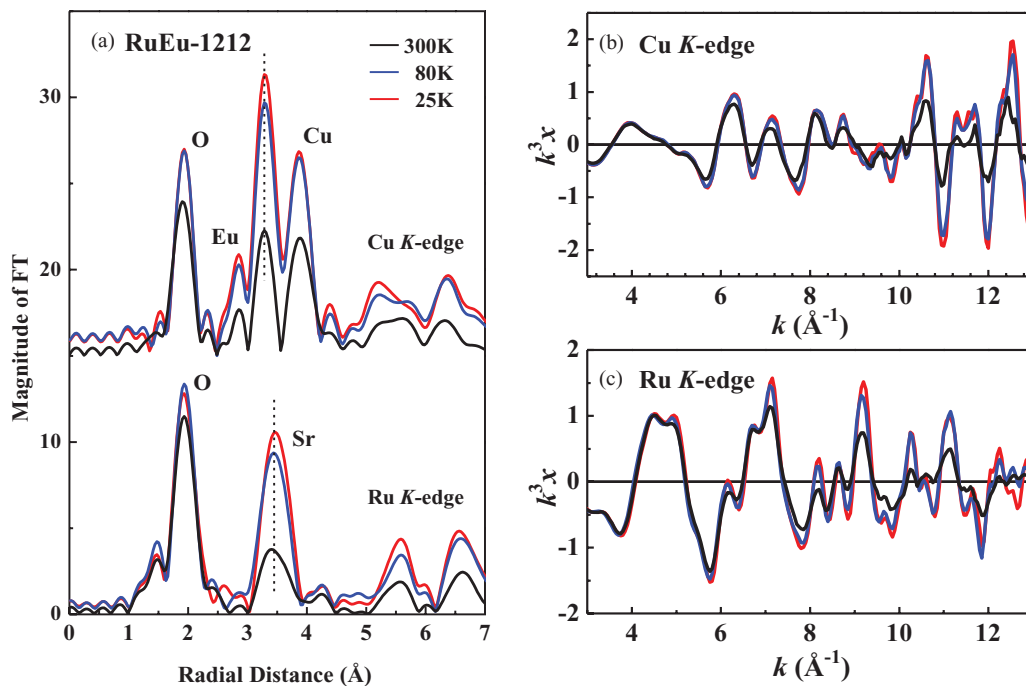

FIG. 7. (Color online) (a) The magnitude of the Cu and Ru K-edge FT spectra in the k ranges of 2.9 to 13.0 Å^{-1} for the Cu K edge and 2.8 to 12.7 Å^{-1} for the Ru K edge at 25 K, 80 K, and RT, respectively. (b) and (c) Their corresponding EXAFS $k^3\chi$ data of RuEu-1212.

correspond to nearest neighbor Cu-O$_{Cu-plane}$ and Cu-O$_{apical}$ (Ru-O$_{Ru-plane}$ and Ru-O$_{apical}$) bond lengths in RuEu-1212, which decrease from low temperatures to RT due to increasing thermal disorder. The FT spectra at Cu and Ru K edges clearly demonstrate that the intensity of the high-shell feature at the Cu (Ru) K edge for the Cu-Sr (Ru-Sr) bond length (indicated by a dashed line) is distinctly enhanced at low temperatures in comparison to that at RT, which indicates an enhancement of the Cu-Sr (Ru-Sr) structural ordering at low temperatures and suggests that the WFM and SC couplings in RuEu-1212 at low temperatures are possibly mediated by Sr-derived states. The WFM and SC couplings can be associated with the Ru t_{2g} states, which do not couple directly with the Cu e_g states but couple indirectly via the apical O p orbitals (or Sr-O$_{apical}$ hybridized sates). The Ru-Sr indirect couplings may strengthen the Ru-Sr structural ordering, as indicated by the observed enhancement of the high-shell feature. Indeed, it has been observed that the nonmagnetic Sr ion played an important role in magnetic transition in SRO.[38] This paper suggests that WFM and SC be accompanied by a significant decrease of local distortions of Cu-Sr and Ru-Sr bonding in RuEu-1212. In order to understand the details of how the dynamic local lattice distortions affect the SC and WFM properties of RuEu-1212, progressive data analysis of the evolution of the local atomic structure with the decrease of the temperature has been underway.[37]

IV. CONCLUSIOIN

In summary, the electronic structures of RuEu-1212 were extensively investigated by XANES at RT, 80 K, and 25 K and by VB-PES at RT. The results indicate that, when the temperature of RuEu-1212 is below T_M, electrons are transferred not only from Cu 3d states but also from Ru 4d states to O 2p orbitals in the Ru-O layers. Additionally, the PSW spectra of the O 2p, Cu 3d, and Ru 4d states derived from VB-PES spectra show that Ru 4d states are much closer to E_f than Cu 3d and O 2p states. It strongly suggests that Ru 4d states are more important in determining the magnetic and electronic properties of RuEu-1212 and provides evidence of a weak overlap between Ru 4d states and strongly Cu 3d-O 2p hybridized states well below E_f, which results in a weak coupling between the CuO$_2$ and RuO$_2$ layers in RuEu-1212. The preliminary result of EXAFS shows that the appearance of WFM and SC is accompanied by a significant decrease of dynamic local lattice distortions of high-shell Cu-Sr and Ru-Sr bonding in RuEu-1212.

*Present address: Department of Physics and Energy Harvest-Storage Research Center, University of Ulsan, Ulsan 680-749, Korea.

†Authors to whom all correspondence should be addressed: dcling@mail.tku.edu.tw; wfpong@mail.tku.edu.tw

‡Present address: National Synchrotron Radiation Research Center, Hsinchu 300, Taiwan.

[1] J. Tallon, C. Bernhard, M. Bowden, P. Gilberd, T. Stoto, and D. Pringle, IEEE Trans. Appl. Supercond. **9**, 1696 (1999).

[2] C. Bernhard, J. L. Tallon, Ch. Niedermayer, Th. Blasius, A. Golnik, E. Brucher, R. K. Kremer, D. R. Noakes, C. E. Stronach, and E. J. Ansaldo, Phys. Rev. B **59**, 14099 (1999).

[3] W. E. Pickett, R. Weht, and A. B. Shick, Phys. Rev. Lett. **83**, 3713 (1999).

[4] Y. Tokunaga, H. Kotegawa, K. Ishida, Y. Kitaoka, H. Takagiwa, and J. Akimitsu, Phys. Rev. Lett. **86**, 5767 (2001).

[5] O. Chmaissem, J. D. Jorgensen, H. Shaked, P. Dollar, and J. L. Tallon, Phys. Rev. B **61**, 6401 (2000).

[6] A. C. McLaughlin, W. Zhou, J. P. Attfield, A. N. Fitch, and J. L. Tallon, Phys. Rev. B **60**, 7512 (1999).

[7] N. M. Souza-Neto, D. Haskel, J. C. Lang, O. Chmaissem, B. Dabrowski, and I. Felner, Phys. Rev. B **80**, 140414(R) (2009).

[8] J. D. Jorgensen, O. Chmaissem, H. Shaked, S. Short, P. W. Klamut, B. Dabrowski, and J. L. Tallon, Phys. Rev. B **63**, 054440 (2001).

[9] L. Bauernfeind, W. Widder, and H. F. Braun, Physica C **254**, 151 (1995).

[10] L. Bauernfeind, W. Widder, and H. F. Braun, J. Low Temp. Phys. **105**, 1605 (1996).

[11] R. S. Liu, L. Y. Jang, H. H. Hung, and J. L. Tallon, Phys. Rev. B **63**, 212507 (2001).

[12] K. Nakamura, K. T. Park, A. J. Freeman, and J. D. Jorgensen, Phys. Rev. B **63**, 024507 (2000).

[13] K. Nakamura and A. J. Freeman, Phys. Rev. B **66**, 140405(R) (2002).

[14] J. S. Kang, J. H. Kwak, Y. J. Shin, S. W. Han, K. H. Kim, and B. I. Min, Phys. Rev. B **61**, 10682 (2000).

[15] J. J. Yeh and I. Lindau, At. Data Nucl. Data Tables **32**, 1 (1985).

[16] B. H. Frazer, Y. Hirai, M. L. Schneider, S. Rast, M. Onellion, U. Asaf, I. Felner, A. Reginelli, L. Perfetti, D. Ariosa, and G. Margaritondo, Phys. Rev. B **62**, 6716 (2000).

[17] K. Asokan, Y. S. Chen, C. W. Pao, H. M. Tsai, C. W. O. Lee, C. H. Lin, H. C. Hsueh, D. C. Ling, W. F. Pong, J. W. Chiou, M. H. Tsai, O. Pena, and C. Moure, Appl. Phys. Lett. **95**, 131901 (2009).

[18] L. Karvonen, M. Valkeapää, R. S. Liu, J. M. Chen, H. Yamauchi, and M. Karppinen, Chem. Mater. **22**, 70 (2010).

[19] K. Fujioka, J. Okamoto, T. Mizokawa, A. Fujimori, I. Hase, M. Abbate, H. J. Lin, C. T. Chen, Y. Takeda, and M. Takano, Phys. Rev. B **56**, 6380 (1997).

[20] J. Park, S. J. Oh, J. H. Park, D. M. Kim, and C. B. Eom, Phys. Rev. B **69**, 085108 (2004).

[21] H. J. Noh, S. J. Oh, B. G. Park, J. H. Park, J. Y. Kim, H. D. Kim, T. Mizokawa, L. H. Tjeng, H. J. Lin, C. T. Chen, S. Schuppler, S. Nakatsuji, H. Fukazawa, and Y. Maeno, Phys. Rev. B **72**, 052411 (2005).

[22] J. Okamoto, T. Okane, Y. Saitoh, K. Terai, S. I. Fujimori, Y. Muramatsu, K. Yoshii, K. Mamiya, T. Koide, A. Fujimori, Z. Fang, Y. Takeda, and M. Takano, Phys. Rev. B **76**, 184441 (2007).

[23]K. Horiba, H. Kawanaka, Y. Aiura, T. Saitoh, C. Satoh, Y. Kikuchi, M. Yokoyama, Y. Nishihara, R. Eguchi, Y. Senba, H. Ohashi, Y. Kitajima, and S. Shin, Phys. Rev. B **81**, 245127 (2010).

[24]H. T. Jeng, S. H. Lin, and C. S. Hsue, Phys. Rev. Lett. **97**, 067002 (2006).

[25]D. J. Singh, J. Appl. Phys. **79**, 4818 (1996).

[26]J. Okamoto, T. Mizokawa, A. Fujimori, I. Hase, M. Nohara, H. Takagi, Y. Takeda, and M. Takano, Phys. Rev. B **60**, 2281 (1999).

[27]J. Park, S. J. Oh, J. H. Park, D. M. Kim, and C. B. Eom, Phys. Rev. B **69**, 085108 (2004).

[28]U. Fano and J. W. Cooper, Rev. Mod. Phys. **40**, 441 (1968).

[29]J. L. Tallon, J. W. Loram, G. V. M. Williams, and C. Bernhard, Phys. Rev. B **61**, R6471 (2000).

[30]N. Tsuda, K. Nasu, A. Fujimori, and K. Siratori, *Electronic Conduction in Oxides*, 2nd ed. (Springer series, Berlin, 2000).

[31]N. Plakida, *High-Temperature Cuprate Superconductors, Experiment, Theory, and Applications* (Springer series, Berlin, 2010)

[32]M. Požek, A. Dulčić, D. Paar, A. Hamzić, M. Basletić, E. Tafra, G. V. M. Williams, and S. Krämer, Phys. Rev. B **65**, 174514 (2002).

[33]A. C. Mclaughlin, J. P. Attfield, R. S. Liu, L. Y. Jang, and W. Z. Zhou, J. Solid State Chem. **177**, 834 (2004).

[34]G. van der Laan and I. W. Kirkman, J. Phys. Condens. Matter **4**, 4189 (1992).

[35]A. Bianconi, N. L. Saini, A. Lanzara, M. Missori, T. Rossetti, H. Oyanagi, H. Yamaguchi, K. Oka, and T. Ito, Phys. Rev. Lett. **76**, 3412 (1996).

[36]C. J. Zhang and H. Oyanagi, Phys. Rev. B **79**, 064521 (2009).

[37]S. W. Han *et al.* (unpublished).

[38]D. Lahiri, T. Shibata, S. Chattopadhyay, S. Kanungo, T. Saha-Dasgupta, R. S. Singh, S. M. Sharma, and K. Maiti, Phys. Rev. B **82**, 094440 (2010).